Proceedings

Eighteenth Annual Symposium

Incremental Motion Control Systems and Devices

B. C. Kuo, Editor

June, 1989

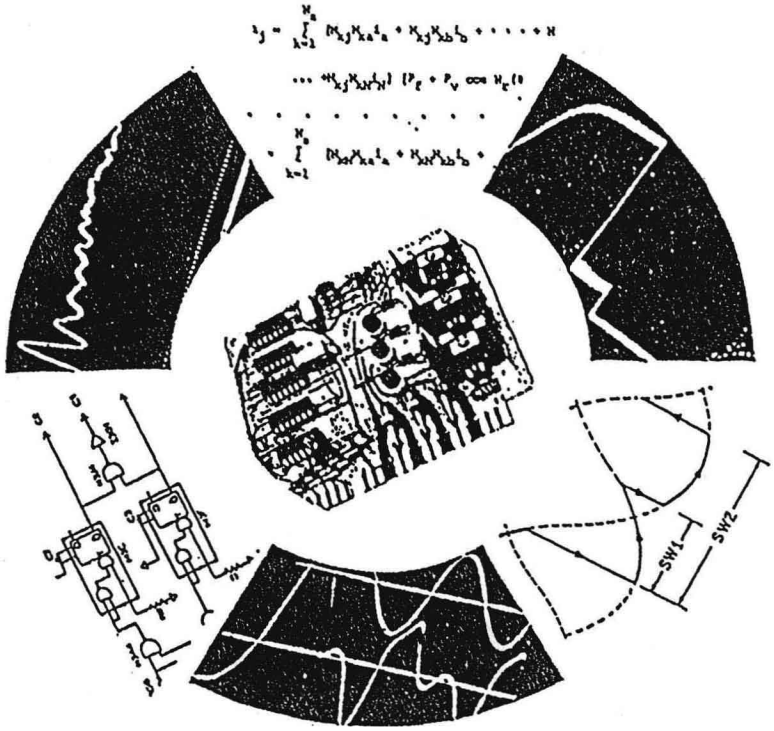

Published by the Incremental Motion Control Systems Society
Post Office Box 2772, Station A, Champaign, Illinois 61825

Library of Congress Catalog Card No. 73-647018

ISBN 0-931538-11-4

ISSN 0092-1661

FOREWORD

The Eighteenth Annual Symposium on Incremental Motion Control Systems and Devices was held at the Chancellor Hotel Convention Center, Champaign, Illinois, June 20-22, 1989. These Proceedings contain the papers presented at the Symposium.

The purpose of the Symposium is to form a forum for scientists and engineers to gather and exchange information and ideas on motion control systems problems.

The editor is indebted to many contributors of this volume. Without their cooperation and efforts, these Proceedings would not have been ready for distribution at the 1989 Symposium.

B. C. Kuo
June, 1989
Champaign, IL, U. S. A.

TABLE OF CONTENTS

AN ASSESSMENT OF VARIOUS MAGNETIC SIMULATION TOOLS

Wade Cole
IBM Corporation
San Jose, CA

H. D. Chai
San Jose State University
San Jose, CA

Introduction

Not numbered among our objectives is any plan to make dogmatic prescriptions for successful computer modelling. What we seek to achieve in this short paper is the sharing of our modelling experience in a development laboratory whose principal mission is design and manufacture of magnetic devices. But the setting in which magnetic design and development is done varies widely. Such variation must be accounted for when assessing computer modelling tools. Moreover, human factors enter each situation and sometimes control whether modelling can be truly effective. Some engineers entertain unrealistic expectations from simulation; others believe only in measurements. The authors choose not to address this imponderable human equation except to plead the case for proper balance between calculation and validation, between simulation and experiment. Also, choice of computing equipment may well be beyond the modeller's control. If only personal computers are available, then choice of developed or purchased simulation software is accordingly limited. The authors have enjoyed the power of a workstation, which includes considerable stand-alone computing power, high resolution graphics and high speed connection to a large mainframe. Cost considerations permitting, a computer workstation is highly recommended for magnetic calculations.

In our view, the best of situations is when each development engineer personally uses modelling tools on computer systems available in his working environment. But it can be argued that (1) not every competent designer is comfortable interacting with computer terminals, and (2) not every modelling program is all that friendly to use, even by an experienced simulation expert. Hence, a sound balance between do-it-yourself modelling and collaboration with simulation experts seems most likely to enhance computer magnetic modelling for product development.

Over time we have grown a magnetic modelling "center of competence." Under its umbrella are maintained an ensemble of simulation programs for use throughout the development laboratory. They range in complexity from simple "early tools" running mainly on PC's to full three dimensional finite element codes that often require a large host machine. Some are "home grown" and distributed internally; others are purchased commercial packages. The expectation is that each engineer will do as much of his own computer modelling as possible. Simulation experts remain available to consult and (when appropriate) to collaborate on a large simulation projects. In this setting, then, we describe computer simulation methods (programs) that we routinely employ for magnetic device modelling.

The Problem to Solve

We restrict our discussion to calculation of static fields and forces. Clearly time varying phenomena are crucial to device modelling and must, in a general sense, be properly addressed. In simplest terms, we seek approximate solutions for the following subset of the celebrated equations of James Clerk Maxwell:

$$\nabla \times \hat{H} = \hat{J} \tag{1a}$$

$$\nabla \cdot \hat{B} = 0 \tag{1b}$$

$$\hat{B} = \mu(H)\hat{H} \tag{2}$$

where $\hat{H}$ is a magnetizing field vector, $\hat{J}$ a current density vector and $\hat{B}$ a flux density vector. μ is permeability of the medium in which field values are to be calculated. H is the magnitude of Hhat.

Flux Circuit Models

Equation 1a may be integrated over some properly smooth open surface S:

$$\int_S \nabla \times \hat{H} \cdot d\hat{S} = \int_S \hat{J} \cdot d\hat{S} \qquad (3)$$

Note that the right hand integral of current density over S results in a total current I enclosed by a boundary curve Γ of S. Stokes' theorem can transform the left hand integral of 3, provided that $\hat{H}$ has continuous first derivatives and Γ enjoys a smoothly turning tangent:

$$\int_S \nabla \times \hat{H} \cdot d\hat{S} = \int_\Gamma \hat{H} \cdot d\hat{\Gamma} \qquad (4)$$

$$\int_\Gamma \hat{H} \cdot d\hat{\Gamma} = I \qquad (5)$$

Equation 5 is simply Ampere's Law asserting that a line integral of H-field around any closed contour equals the current enclosed. If a given magnetic situation confines most of its magnetic flux to highly permeable material and specified air gaps, then 5 provides a sound basis for estimating magnetic parameters. Pursuant to that, consider rewriting 5 in terms of $\hat{B}$ instead of $\hat{H}$, using 2:

$$\int_\Gamma \frac{\hat{B} \cdot d\hat{\Gamma}}{\mu\mu_0} = I$$

in which μ is taken to mean relative permeability and μ_0 is the permeability of free space. Dividing a configuration of iron and air into pieces, each with prescribed length and cross sectional area, provides a basis for representing the integral above as an approximating sum. Such a sum is,

$$\sum_{i=1}^{n} \frac{\Phi_i L_i}{\mu\mu_0 A_i} = I \qquad (6)$$

in which Φ_i is magnetic flux (product of B and area), L_i is length and A_i is cross sectional area of the i th piece. For n pieces, an analyst must prescribe n independent loops in order to imply n linearly independent equations which may be solved for the Φ_i. Observe that, if 2 applies as written, the equations are non-linear: matrix coefficients (the branch reluctances) will depend on B-H properties of material composing the branches. Right hand sides will be applied mmf (eg. in amperes), either from current in windings or from magnets in the loops. Magnets, of course, may introduce additional non-linearity into the situation.

It has long been practice to obtain estimates for magnetics problems by using a "lumped parameter" approach as described above. Working by hand an analyst views the topology of his magnetic circuit and "writes down" branch equations from loops he traces out by eye. In so doing, he can see how many unknowns are required, namely, as many unknowns as there are independent loops. Often, by visual inspection, problems may be greatly simplified and the number of unknowns and equations reduced (sometimes dramatically) by recognizing particular features of the given situation.

We chose to implement this flux-circuit model as general purpose computer programs. It is difficult to match the ability of a human being to recognize independent loops in a circuit. Hence, instead of solving branch equations it proves convenient to solve nodal equations. Viewed in terms of its nodes, any magnetic circuit provides just one equation and one unknown for each node. For every node except one, such an equation (for the j th node) is of the form,

$$\sum_{i=1}^{k} P_{ij}(u_j - u_i) = \Phi_{aj} \qquad (7)$$

in which P_{ij} is permeance of that branch joining i th and j th nodes, and u represents node potential (mmf). Φ_{aj} represents prescribed flux from branches with windings or magnet branches connected to node j. Equation 7, which denotes k branches connected to node j, is purely

formal and does not reflect a finished situation in which all nodes and branches have been properly numbered and a corresponding coefficient matrix defined.

We have described the flux circuit model in some detail because we find it to be a powerful tool when available as easy-to-use computer programs. Flux circuit modelling by a skilled designer can be astoundingly effective (Ref. 7) Magnetic simulation software based on the flux circuit model embodies concepts familiar to magnetics designers, is cost effective to prepare and apply and well serves as convenient checkpoints for results from other more complex modelling techniques.

We developed three flux circuit programs, namely, Maxboe, Maxnet and Maxslv. Maxboe is a full screen interactive magnetics formula evaluator and units tracker. Maxnet provides a full screen interactive vehicle for defining flux circuit models and Maxslv calculates linear/nonlinear solutions of generated networks. Personal computer solution times for flux circuit networks rarely exceed a few seconds to several minutes. It becomes possible, therefore, to try many configurations and materials for early design steps or make quick independent checks of data from other solution methods.

Finite Element Models

To fulfill objectives of this paper we sketch just one possible derivation of a finite element method as applied to magnetostatic simulation. Under assumption that sources of $\hat{H}$ are localized (eg. in current carrying conductors) a total $\hat{H}$ can be expressed as the sum of that due to sources and that due to stray field from magnetized material:

$$\hat{H} = \hat{H}_a + \hat{H}_m$$

The $\hat{H}_m$ field has zero divergence and curl, that is,

$$\nabla \cdot \hat{H}_m = 0$$

$$\nabla \times \hat{H}_m = 0$$

which implies existence of a magnetic scalar potential function U satisfying,

$$-\nabla \cdot (\mu \nabla U) + \nabla \cdot (\mu \hat{H}_a) = 0 \qquad (8)$$

from which $\hat{H}_m$ may be calculated as a gradient:

$$\hat{H}_m = -\nabla U$$

Solving equation 8 by a finite element method requires subdividing (meshing) a prescribed "solution space" into contiguous subregions over each of which the unknown potential function may be adequately represented by simple algebraic functions, say polynomials of degree one or two. Not only that, but other sometimes tedious and vexing details must be attended to, such as prescribing proper conditions on boundaries of the solution space. Two dimensional meshing may at least be semi-automatic. Three dimensional meshing is harder. All these matters of data preparation are done in a preprocessing step, like preparing the flux circuit network noted above. After an associated FEM solver has calculated potential values (U) at the meshed nodes, a postprocessing step is typically employed to calculated fields or other parameters of interest to the modeller. On balance, it should be plainly stated that in spite of substantial progress toward making FEM magnetic modelling software easier to use, such programs still require a fair amount of understanding, patience and skill to employ. Even such things as whether nonlinear iterations are converging, whether Newton steps or simple update iterations are going to work best in a given situation become a concern of the FEM user. That is the bad news. The good news is that (where appropriate) full nonlinear three dimensional FEM analyses can provide excellent estimates of gap flux, B-H situation in iron parts, operating points of magnets, and the like. In contradistinction to the flux circuit model, FEM can also provide good estimates of stray fields in air surrounding magnetic material, which may be crucial in compact design situations.

Boundary Element Models

The general magnetostatic problem may also be formulated as a Fredholm integral equation of the second kind:

$$(\mu + 1)U(s) = \frac{(\mu - 1)}{\pi} \int_S K(s,t)U(t)dt + 2U_a(s) \quad (9)$$

where U(s) is a magnetic scalar potential, S is a boundary of magnetic material whose relative permeability is μ and K(s,t) is a prescribed function whose form depends on details of formulation and on whether there are two or three space dimensions. U_a is an applied potential from current in conductors or from permanent magnets in the neighborhood of magnetic material. Solving equation 9 gives distribution of potential on material surface. Companion formulas define the potential everywhere else, so that distribution of field may be calculated.

Typically, using BEM software is easier than FEM software. First, the dimension of the original problem is reduced by one. This means that for a magnetostatic situation in two dimensions, the modeller must only "mesh" simple closed curves bounding regions of iron. In three dimensions only two dimensional surfaces of material must be meshed. Recall that in FEM meshing all of solution space is required. For BEM only iron surfaces need be meshed. One price of this simplification is that permeability of the iron remains constant in the interior. Some BEM implementations provide optional interior meshing to permit estimating volume divergence of field. Second, general boundary conditions for solution space need not be prescribed as these are accounted for in the solution formulation. In all, problem preparation, such as meshing and other attendant details, are not as demanding for BEM as for FEM magnetic software.

Making Sure Answers are Right

In the world of American jurisprudence an accused is innocent until proven guilty: in magnetic simulation an answer is wrong until proven correct. In our experience all effort expended to establish correctness is well spent indeed. We see three ways to establish correctness, namely (1) compare with measurement, (2) calculate results in more than one way and (3) assure that answers are self-consistent. Experience keeps a dear school: we have learned not to believe automatically that measurements are correct. Rather, we try to balance measurement and calculation in an even-handed manner.

By way of illustration we include Figure 1. It shows comparisons of calculation and measurement for a simple current energized iron yoke with narrow air gap.[1] Gap field was calculated by flux circuit, BEM and FEM models and compared with measurement. Since flux is confined to iron and narrow gap, the flux circuit model provides a salutary result. But the other models can also show how field varies in gap and iron and provide estimates of stray field in the neighborhood of the device. For the particular case reported in the table, we must ponder, however briefly, why the flux circuit estimate is actually closer to measurement than either of the others.

Flux Circuit	2d BEM	3d FEM	Measured Value
.495 T	.486 T	.465 T	.510 T

Figure 1. Gap Field Comparisons in Test Yoke

Purchasing Simulation Software

During the past decade or so the number of commercially available magnetic simulation software products has increased dramatically. It is impossible to decide from an advertising brochure whether a particular offering can do the work the modeller intends for it. Here are some practical considerations for making a selection:

1. All magnetic simulation software is not created equal. Beyond the broad distinctions in formulation sketched above there are further differences in capabilities, graphics, documentation, support and cost. Even methods of charging for use and copy-protecting the software can range from easy to accept to onerously inconvenient. These often vexing matters of detail should be well in hand before making a decision to buy.

2. By all means, arrange for more than a simple demonstration. Money spent for a one to three month trial lease is well spent. Of particular importance, especially for three dimensional modelling, are preprocessing (data preparation) and postprocessing (results presentation) facilities. Only by running

case after carefully selected case can the prospective buyer tell whether software designers realistically perceived how happily a human being would fare while using their creation.

3. Assure that the vendor will provide accessible, friendly and competent consultation service with the product.

Epilogue

Finally, we include the following table of magnetic simulation software we currently employ. For the future we anticipate additional entries in such a table to meet the ever growing and changing simulation requirements of our laboratory.

Program	*Description and Status*
Flux Solver	Flux circuit solver as described above. Distributed for personal use on PC's around the development laboratory.
2d-BEM (1)	Two dimensional boundary element magnetic solver. Heavily used over several years through terminals attached to large host machines.
2d-BEM (2)	Two dimensional linear/nonlinear magnetic solver for PC.
3d-FEM	Full nonlinear three dimensional magnetic/electrostatic solver with high resolution pre- and post-processing graphics.
3d-BEM	Three dimensional (linear) boundary element program for use on workstation/host with companion pre- and post-processor.

References

1. Lectures on Electromagnetic Theory, L. Solymar, Oxford University Press, Oxford, 1976.
2. A Microprocessor Based Electromagnetic Field Analysis System, D. A. Lowther, IEEE Trans. on Magnetics, Vol. Mag-18, No. 2, March 1982.
3. Three-dimensional nonlinear electromagnetic, field computations using scalar potentials, J.Simpkin and C.W.Trowbridge, IEE Proc. Vol 127, Pt. B, No. 6, November 1980.
4. Finite Elements in Electrical and Magnetic Field Problems, M.V.K. Chari and P.P. Sylvester, eds., John Wiley and Sons, New York, 1980.
5. Integral Equation Methods in Potential Theory, and Electrostatics, M. A. Jaswon and G. T. Symm, Academic Press, London, 1977.
6. Developments in Boundary Elements-1 (and -2), P.K. Bannerjee and R. Butterfield eds., Applied Science Publishers, London, 1979.
7. Brushless DC Motors: Torque and Inductance Determination, Proc. IMCSD, 1987, Champaign, Ill.

[1] The authors are grateful to R. W. Lissner and B. Barcarse for permission to use these data.

The Design of A Minimum-Power VCM for A Very Short Seek Time

Wen-Wei Chiang
Robert Mizrahi

IBM Research Division
Almaden Research Center
San Jose, California 95120

ABSTRACT

This paper describes in detail how a voice coil motor (VCM) was dimensioned for use in a rotary actuator test system. The design of this VCM conforms to the requirement of a very short seek time (7 msec) with a minimum amount of power.

This paper complements two other papers previously published by the primary author which present a theoretical analysis for the optimization of a motor design.[1,2] A person without much previous experience will be able to start designing high performance VCM's by following the procedures in these papers.

INTRODUCTION

Previous research by the primary author[1] resulted in a systematic analysis of the performance parameters of any D.C. motor which operates under constant voltage and has to start and stop in a given time (seek time). The optimal design point to achieve the minimal seek time with a fixed amount of power, or vice versa, can be determined directly once load inertia and displacement are specified. Another paper by the primary author[2] also described how the three primary design parameters: power dissipation, power rate,[3] and motor coil location, are determined for the VCM of a magnetic disk drive rotary actuator test system which achieves a 7 msec average move time.

After the authors developed the theoretical analysis, it became important to demonstrate how the latter can be used to develop a piece of hardware, and to verify experimentally the accuracy of the theory. This paper describes in detail how those primary design parameters are converted to mechanical dimensions of a VCM and its test system.

REVIEW OF PREVIOUS RESULTS

Previous analysis result[1] indicated that under a constant voltage seek profile, the seek time decreases as the motor torque constant, or the power rate, increases when increasing the magnetic field, and the gear coupling ratio should be set according to that to minimize the seek time. However, there exists an asymptotic limit for the seek time as the torque constant increases. High magnetic field also create high back EMF, which limits the maximum motor speed at a constant voltage. Therefore, an optimal DC motor should be designed with the proper amount of magnetic field when the effect of further increased field strength in reducing the seek time starts to decrease.

A dimensionless contour plot showing the normalized seek time (t_f / β) as a function of the motor characteristic α and the normalized gear coupling ratio γ, is shown in Figure 1. It was developed from that study and indicates the relations between the three motor design parameters. The study indicated that the optimum design is obtained for $1 < \alpha < 2$ and $0.6 < \gamma < 1$.

DESCRIPTION OF EXPERIMENTAL SETUP

A 3.5" magnetic disk rotary actuator test system was designed to test the mechanical behavior of the actuator driven by a VCM. It was also intended to test the VCM in order to check the theoretical analysis on which its design was based.

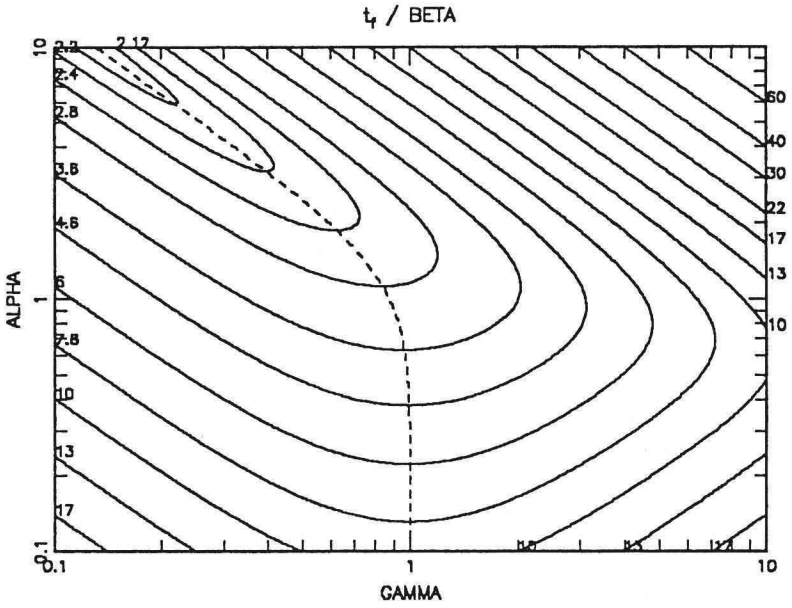

Figure 1: Solid contour lines indicate normalized move time t_f / β, and the dotted line shows the optimal coupling ratio γ^* for each value of the motor characteristic α.

Design Goal

The test system has a rotary actuator with two arms each of which holds a suspension and slider assembly which accesses either side of a single 3.5" rigid magnetic disk. The goal of the design is to develop a VCM with sufficient torque for moving the actuator in 7 msec, excluding settling time, over one third of the data band width which is considered to be the average track seek distance.

Load Condition

The lengths of the two actuator arms was chosen to position the read/write head at 54 cm from the actuator pivot axis, their thickness and width were chosen so that its natural frequency would be higher than 2 KHz. Since their size is set, so is their inertia which is the main component of the inertial load on the VCM, excluding that of the coil. This load was estimated to be 1.84×10^{-6}kg-m^2. The data band is 19 mm wide for a typical 3.5" disk drive. It follows that the angular displacement of the rotary actuator should be 0.35 radian, and one third of which (0.116 radian) is conventionally called the average seek distance.

VCM Design

One of the previous papers[2] has described in detail how the three primary parameters : power, power rate, and coil location are determined. For our tester we calculated that the the VCM needs 1.82 watts of power, a power rate of 905 watts/sec at the start of the seek when the velocity is zero, and must have the center of the two active lengths of its coil located at 20 mm from the actuator pivot.

Coil Assembly Design

It was decided to wind the wire on a TORLON core; it can withstand a temperature of 200°C and has a specific gravity of 1.4. Aluminum wire was chosen for its lower mass density and electrical resistivity product value over copper alloys. 1.82 watts of power requires 0.158 ampere of current if 11.52 volts is applied to

the coil, and the coil has to provide 72.9Ω of resistance to match the voltage and current. Using the empirical current density 12.5A/mm^2, it is found that 5 mils of diameter (36 AWG) is required for the round aluminum wire. From the resistance per unit length of the wire, and assuming 30% increase of the resistance when the coil heats up during operation, it is found that the total length of the wire should be 26.8 meters, and the total mass of the aluminum wire used for each coil is 9.03×10^{-4}kg.

The total volume occupied by the aluminum wire when making the coil assembly is calculated by assuming that each circular cross section of the wire occupies a rectangular space with each side equal to the diameter of the wire plus coating thickness (0.147 mm), and additional 30% of void space is needed for the epoxy to fill in when "random wound" method is employed. The "random wound" method is employed because "layer wound" is impractical for the pancake-shaped flat coil design. Therefore, the total coil volume occupied by the wire is calculated as $(1.47 \times 10^{-4})^2 \times 26.8 \times 1.3$ and it is 7.53×10^{-7}m^3, or 753mm^3.

A pancake-shaped flat coil geometry design is chosen, and its geometry is shown in Figure 2. The coil has a trapezoidal shape, with the center of the two active lengths at 20 mm from the actuator pivot axis. The two converging sides, which are located in the magnetic gap, are separated by 0.52 radian to provide enough angular stroke for the actuator to cover the whole data band (0.35 radian), plus some margins to avoid the edge of the magnetic gap where the magnetic field is weakened by leakage. The converging ends of the

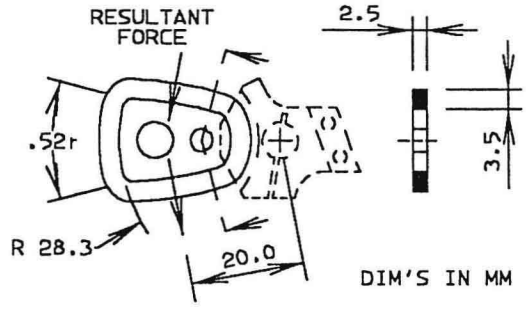

Figure 2: Top view and cross section of the VCM coil assembly.

coil is 11.66 mm away from the actuator pivot axis so that enough space is left for the bearings in the actuator hub. The length of each turn of the wire is found to be 60.4 mm, and a total number of 444 turns can be calculated based on the total wire length of 26.8 meters.

The coil cross section can be calculated by dividing the total volume occupied by the wire and epoxy, by the length of each turn as 753 / 60.4 = 12.5mm^2. The width (along the coil radial direction) and the thickness (along the coil axial direction) of the coil should have a product equal to the cross section area just calculated. A smaller thickness requires a thinner magnetic gap, but it results in a wider coil, which requires a larger area of the magnetic gap. Therefore, the coil's cross section dimensions should be such as to minimize the size of the magnet, and still conform to the space constraint. These dimensions should also be chosen so that the coil can be manufactured easily. For this design we chose a thickness of 2.5 mm and a width of 5.0 mm. The fabricated coil had 444 turns and measured 2.5 x 3.5 mm as shown in Figure 2.

Magnet Assembly Design

Previous analysis estimated that the the total moment of inertia of the VCM coil and its core is 6.77×10^{-7}Kg-m^2 when the active lengths of the coil are located 20 mm from the actuator pivot axis. In order to develop 905 watts/sec of power rate with 0.158 ampere of current at the beginning of each seek, the motor torque constant has to be 0.157 N-m/Amp. The active length of the coil which is acted upon by the magnetic field is roughly 53.2% of the total length of the coil. Consequently, it can be found that the field strength required is 5.5 K Gauss. Allocating 4 mm for the gap, and assuming the remanence of the NdFeB magnet to be 10 K Gauss, it is found that each of the magnets located on either side of the coil, should be 2.5 mm thick. Two pairs of such magnets are required to create two zones with opposite magnetic field direction, each for one side of the VCM coil, so that torques produced by these two sides are in the same direction. Figure 3 shows the top and end views of the magnet assembly design.

Back and side iron plates are required to direct the returning magnetic flux. The magnetic saturation level for iron is 13 K Gauss, and the thickness of iron plates should be chosen to avoid saturation. Assuming half

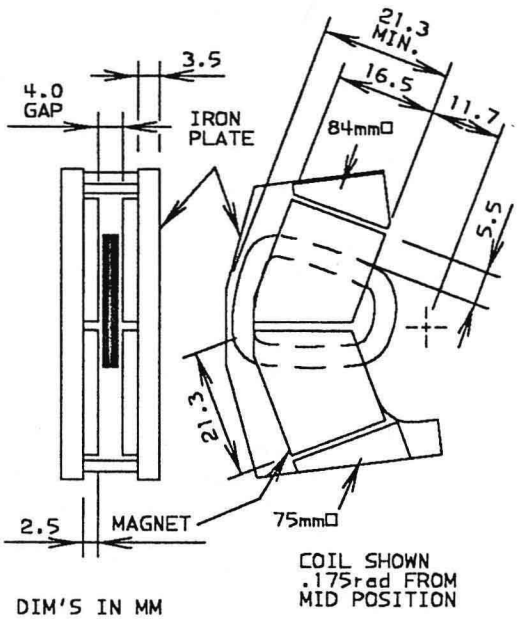

Figure 3: Top view and cross section of the magnet assembly.

of the magnetic flux is returned from top to bottom of the gap through the side iron plate, and half is returned from left to right through the back iron plate, then multiplying the cross section area of the gap by 5.5 K Gauss gives the total flux, and half of it should be divided by 13 K Gauss to give the cross section area of the side and back iron plates. Therefore, their cross section area should be $(21.3 \times 16.5) \times 5.5 / (2 \times 13) = 74.4 mm^2$, which means the back iron plates should be $74.4 / 21.3 = 3.5 mm$ thick.

Test System Mechanical Design

All the dimensions given for the coil, hub, arms, suspensions, and magnet assembly were such as to allow two actuators to fit side by side in the standard 3.5" disk file envelope (145 × 100 × 40 mm). Since the actuator was going to be driven back and forth constantly without a stop for a change in direction, the rotating mass would have to have a bearing stiffness large enough to obtain a natural frequency two to three times that of the driving frequency (1 / (2 × 7 msec) = 71 Hz). The shaft had a diameter of 6 mm, the bearings were set far apart and had an axial preload of 1.5 Kg. They were set on either side of the actuator. One bearing was embedded in the base plate, the other one set in a heavy bridge fastened to the same base plate.

The hub was shaped like a clamp so that its location on the pivot could be set to suit the exact height of the disk above the base plate. Two copper strips were connected to the two ends of the coil and were set on a strip of polyimide fastened to the hub. Room for the curling and uncurling of the strip had to be gouged out of the base of the bridge. Figure 4 shows an isometric drawing of the test system, with the top of the magnet assembly raised to show the inside of the VCM.

TEST RESULTS

Some parameters of the VCM built are measured and compared with their design values, and they are listed in the following table:

Parameter (unit)	*Actual*	*Design*
Resistance (Ω)	75	72.9
Current (Amp)	0.16	0.158
Power (watts)	1.92	1.82
Total wire length (m)	33	26.8
Wire in gap (%)	45	53.2
Wire in gap (m)	14.8	14.3
Gap field (K Gauss)	5.4	5.5
Load M.O.I. (10^{-6}kg-m^2)	1.91	1.84
Motor M.O.I. (10^{-6}kg-m^2)	0.56	0.68
Power rate (watts/sec)	1245	905
α	1.24	1.09
β(msec)	2.37	2.39
γ	0.54	0.607

The moment of inertia were not measured but calcu-

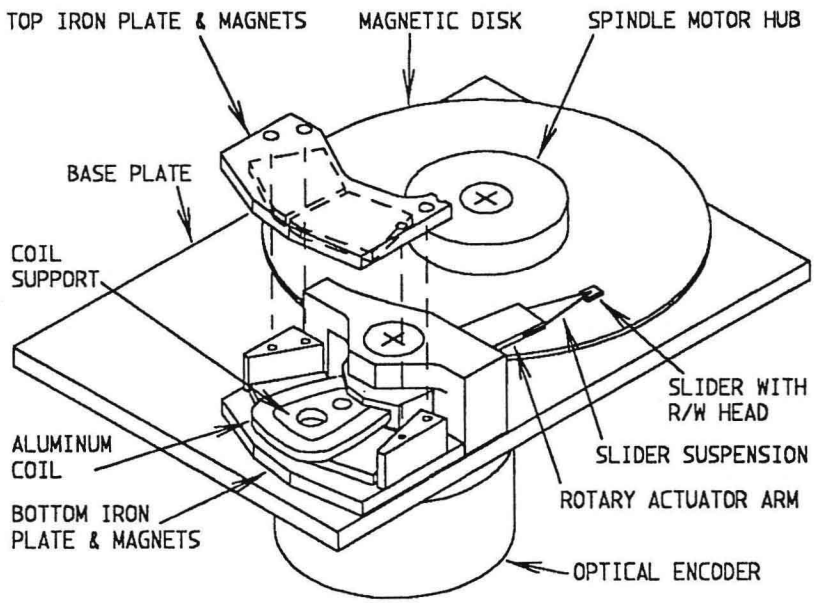

Figure 4: Assembly drawing of the 3.5″ disk drive actuator/VCM test system, achieving 7.2 msec move time for average seek.

lated from the CAD drawings because of the difficulty in measuring them. The table above shows that the actual test system did not deviate too much from the original design. The total wire length is calculated based on the coil resistance at room temperature and the wire's resistivity per unit length. The actual total length 33 meters is more than the design value of 26.8 meters because radii of curvature of the wire around corners get larger as the coil layer grows wider in the radial direction, which also cause less percentage of the wire to be located in the gap. However, the total absolute length of wire located inside the magnetic gap is still the same, and the total amount of torque produced is not affected.

12 V D.C. with alternating polarities was applied to the VCM coil to test the actuator speed during seek. An optical encoder disk was attached to the rotating shaft to measure the angular displacement. The encoder signal is fed back with a small gain to the VCM driver to prevent the actuator from drifting away from the desired range of motion.

The period of the alternating D.C. voltage is adjusted to obtain 0.116 radian peak-to-peak angular displacement. Test results are recorded on a storage oscilloscope, and are shown in Figure 5. They indicate that

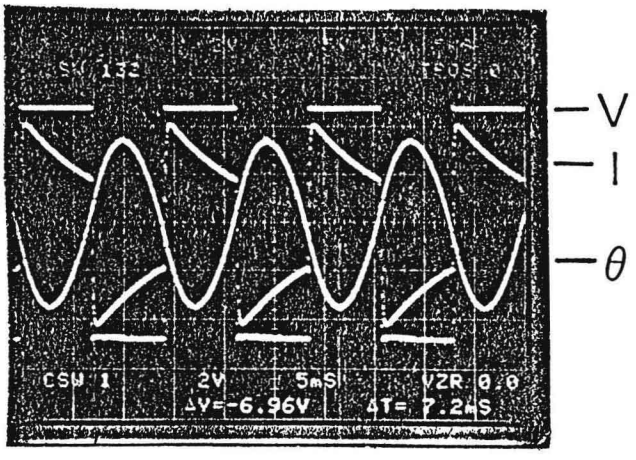

Figure 5: Test results of the 3.5″ rotary actuator/ VCM test system, showing the alternating constant coil voltage (V), coil current (I), and angular position (θ). 7.2 msec is required to move between extreme positions.